ISSN 1063-7842, Technical Physics, 2021, Vol. 66, No. 3, pp. 369–375. © Pleiades Publishing, Ltd., 2021.
Russian Text © The Author(s), 2021, published in Zhurnal Tekhnicheskoi Fiziki, 2021, Vol. 91, No. 3, pp. 351–387.

THEORETICAL AND MATHEMATICAL PHYSICS

The Problem of the Shape of a Vertical Liquid Bridge between Convex Surfaces Taking the Gravity Force into Account

E. V. Galaktionov[a,*], N. E. Galaktionova[b], and E. A. Tropp[a]

[a] *Ioffe Institute, St. Petersburg, 194021 Russia*

[b] *Peter the Great St. Petersburg Polytechnic University, St. Petersburg, 195251 Russia*

**e-mail: evgalakt@mail.ru*

Received May 20, 2020; revised September 27, 2020; accepted September 29, 2020

Abstract—The solution to the problem of the shape of the lateral surface of a vertical 3D catenoidal liquid bridge of small volume between two arbitrary convex solid surfaces in the axisymmetric case taking into account the gravity force is presented. A variational formulation of the initial problem is given. The solution is found by the iteration method under the assumption of a small Bond number. An algorithm of the iterative process is proposed. We have detected domains of variation of parameters in which the uniqueness of the solution is not observed. It is found that the maximal number of different lateral surface profiles of the liquid bridge, which correspond to a single chosen set of parameters, is four. By way of example, the problem of the liquid bridge shape between two spheres is solved.

DOI: 10.1134/S1063784221030075

INTRODUCTION

In our earlier publications [1, 2], the problem of the shape of a vertical catenoidal liquid bridge between two solid horizontal planes was solved. Such a problem appears, in particular, in analysis of the shape of liquid meniscuses formed during the crystal growth by the Stepanov method [3]. However, the crystallization front in this process is known to be not flat, but a small-curvature convex surface. For this reason, the problem of the shape of a liquid bridge between two arbitrary convex solid surfaces is topical. Problems of this type are solved using both numerical and asymptotic methods. The asymptotics of the surface shape of the horizontal liquid bridge between two solid vertical planes was constructed in [4] for small Bond numbers. In [5, 6], an original approach to determining the shape of a liquid bridge between two spheres was proposed based on the solution of the inverse problem. The classification of the shapes of liquid bridges was given in [5], while their experimentally obtained photographs are presented in [6]. Numerous publications devoted to solution of the liquid bridge shape problem and possible applications of the results of these studies were given in [7].

In this study, we consider a variational formulation of the problem of the shape of the lateral surface of a vertical 3D catenoidal liquid bridge of a small volume between two arbitrary convex solid surfaces. The axisymmetric case is considered, and cylindrical coordinates are used to solve the problem. The effect of gravity is taken into account. It is assumed that the Bond number is a small parameter of the problem. An algorithm of the iterative process is proposed. By way of example, a solution to the problem of the shape of a liquid bridge between spheres is considered.

1. VERTICAL LIQUID BRIDGE. VARIATIONAL FORMULATION OF THE PROBLEM

Let us consider a vertical liquid bridge between two solid convex surfaces (bottom and top; Fig. 1). In view of the presumed axial symmetry, we will solve the problem of determining the profile of the lateral surface of the liquid bridge in cylindrical system of coordinates (r, z). Surface tensions between the media are α_{13}, α_{14}, α_{34}, α_{23}, and α_{24}, respectively. The region of contact of the liquid bridge with surface $z = f_1(r)$ $(f_1(0) = 0)$ (bottom) is a circle of radius r_1, while the region of contact with surface $z = \hat{f}_2(r) = \hat{h} + f_2(r)$ $(f_2(0) = 0)$ (top) is a circle of radius r_2. We denote by $u_1(r)$ and $u_2(r)$ the sought functions describing the profiles of the lower $(u_1(r))$ and upper $(u_2(r))$ parts of the lateral surface of the liquid bridge. The region (neck) separating these parts is a circle of radius r_* $(r_* \geq 0)$. In this study, we consider a catenoidal liquid bridge [8]: $r_* < \min\{r_1, r_2\}$, $u_1'(r) < 0$, $r \in [r_*, r_1]$, $u_2'(r) > 0$, $r \in [r_*, r_2]$. In addition, we assume that angles θ_1 and θ_2 satisfy the following conditions: $0 < \theta_i < \pi/2 - \arctan|f_i'(r_i)|$, $i = 1, 2$; i.e., the liquid wets the solid surfaces [3]. Since there are no physical reasons for sharpening of the liq-

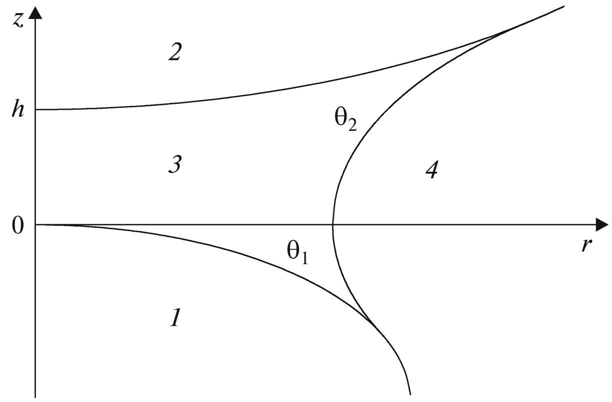

Fig. 1. Vertical axisymmetric liquid bridge between two solid convex surfaces: (*1*, *2*) solid media, (*3*) liquid medium, and (*4*) gaseous medium; θ_1 and θ_2 are wetting angles.

uid bridge profile, the tangent to the profile at the point with abscissa $r = r_*$ must be vertical: $u_1'(r_*) = -\infty$, $u_2'(r_*) = +\infty$, and $u_1(r_*) = u_2(r_*)$. It should be noted that, because of the aforementioned constraints, functions $u_1(r)$ and $u_2(r)$ are single-valued.

We assume that the volume of the liquid bridge is fixed:

$$I\{u_1(r),u_2(r)\} = 2\pi\left(\int_{r_*}^{r_1}(u_1(r)-f_1(r))rdr + \int_{r_*}^{r_2}(\hat{f}_2(r)-u_2(r))rdr\right) + 2\pi\left(\int_0^{r_*}(\hat{f}_2(r)-f_1(r))rdr\right) = V. \quad (1)$$

Let us introduce a functional that includes the surface energy and the energy of the gravity force. The surface energy then, in turn, consists of a component that corresponds to the free surface of the liquid bridge and components that corresponds to its contact with the solid. The functional in question can be written in the form

$$J\{u_1(r),u_2(r)\} = 2\pi\int_{r_*}^{r_1}\left\{\alpha_{34}\sqrt{1+(u_1')^2} + \frac{1}{2}g\rho(u_1-f_1)^2 + (\alpha_{13}-\alpha_{14})\sqrt{1+(f_1')^2}\right\}rdr$$
$$+ 2\pi\int_{r_*}^{r_2}\left\{\alpha_{34}\sqrt{1+(u_2')^2} - \frac{1}{2}g\rho(\hat{f}_2-u_2)^2 + (\alpha_{23}-\alpha_{24})\sqrt{1+(f_2')^2}\right\}rdr \quad (2)$$
$$+ 2\pi\int_0^{r_*}\left\{(\alpha_{13}-\alpha_{14})\sqrt{1+(f_1')^2} + (\alpha_{23}-\alpha_{24})\sqrt{1+(f_2')^2} + \frac{1}{2}g\rho(\hat{f}_2-f_1)^2\right\}rdr,$$

where g is the acceleration due to gravity and ρ is the density of the liquid. Thus, we have obtained the following isoperimetric problem: finding the minimum of functional (2) provided that functional (1) takes a preset value V. In accordance with the Euler theorem on isoperimetric problems, we introduce an expanded functional (λ is a Lagrange multiplier):

$$J\{u_1(r),u_2(r)\} + \lambda I\{u_1(r),u_2(r)\} = 2\pi\int_{r_*}^{r_1}H_1(r,u_1(r),u_1'(r))dr \quad (3)$$
$$+ 2\pi\int_{r_*}^{r_2}H_2(r,u_2(r),u_2'(r))dr + 2\pi\int_0^{r_*}H_3(r)dr,$$

where

$$H_1 = \left\{\alpha_{34}\sqrt{1+(u_1')^2} + \frac{1}{2}g\rho(f_1-u_1)^2 + (\alpha_{13}-\alpha_{14})\sqrt{1+(f_1')^2} + \lambda(u_1-f_1)\right\}r,$$

$$H_2 = \left\{\alpha_{34}\sqrt{1+(u_2')^2} - \frac{1}{2}g\rho(\hat{f}_2-u_2)^2 + (\alpha_{23}-\alpha_{24})\sqrt{1+(f_2')^2} + \lambda(\hat{f}_2-u_2)\right\}r,$$

$$H_3 = \left\{\frac{1}{2}g\rho(\hat{f}_2-f_1)^2 + (\alpha_{13}-\alpha_{14})\sqrt{1+(f_1')^2} + (\alpha_{23}-\alpha_{24})\sqrt{1+(f_2')^2} + \lambda(\hat{f}_2-f_1)\right\}r.$$

By varying the extended functional, we obtain two Euler equations and two transversality conditions. Let us introduce dimensionless variables $\xi = r/V^{1/3}$, $w_i(\xi) = u_i(r)/V^{1/3}$, $i = 1, 2$; $\varphi_1(\xi) = f_1(r)/V^{1/3}$, $\hat{\varphi}_2(\xi) = \hat{h}/V^{1/3} + f_2(r)/V^{1/3} = h + \varphi_2(\xi)$ and dimensionless parameters $\mu = \lambda V^{1/3}/\alpha_{34}$ and $B = g\rho V^{2/3}/\alpha_{34}$. Dimensionless constant B is the Bond number.

In dimensionless form, the problem includes the Euler equations for the lower and upper branch, respectively:

$$\frac{d}{d\xi}\left(\frac{\xi w_1'(\xi)}{\sqrt{1+(w_1'(\xi))^2}}\right) = B\xi(w_1(\xi)-\varphi_1(\xi)) + \mu\xi, \quad \xi_* < \xi < \xi_1, \quad (4)$$

$$\frac{d}{d\xi}\left(\frac{\xi w_2'(\xi)}{\sqrt{1+(w_2'(\xi))^2}}\right) = B\xi(\hat{\varphi}_2(\xi) - w_2(\xi)) - \mu\xi, \quad \xi_* < \xi < \xi_2; \tag{5}$$

transversality conditions

$$\frac{1+\varphi_1'(\xi_1)w_1'(\xi_1)}{\sqrt{1+(w_1'(\xi_1))^2}} = \alpha_{10}\sqrt{1+(\varphi_1'(\xi_1))^2}, \quad \alpha_{10} = \frac{\alpha_{14}-\alpha_{13}}{\alpha_{34}}, \tag{6}$$

$$\frac{1+\varphi_2'(\xi_2)w_2'(\xi_2)}{\sqrt{1+(w_2'(\xi_2))^2}} = \alpha_{20}\sqrt{1+(\varphi_2'(\xi_2))^2}, \quad \alpha_{20} = \frac{\alpha_{24}-\alpha_{23}}{\alpha_{34}}; \tag{7}$$

conditions of contacts of the bridge with the bottom and top,

$$w_1(\xi_1) = \varphi_1(\xi_1), \tag{8}$$

$$w_2(\xi_2) = h + \varphi_2(\xi_2); \tag{9}$$

continuity condition for the profile in the neck,

$$w_1(\xi_*) = w_2(\xi_*); \tag{10}$$

verticality conditions for the tangent in the neck,

$$w_1'(\xi_*) = -\infty, \quad w_2'(\xi_*) = +\infty; \tag{11}$$

and volume conservation condition,

$$2\pi\left(\int_{\xi_*}^{\xi_1}(w_1(\xi)-\varphi_1(\xi))\xi d\xi + \int_{\xi_*}^{\xi_2}(\hat{\varphi}_2(\xi)-w_2(\xi))\xi d\xi\right) + 2\pi\left(\int_0^{\xi_*}(\hat{\varphi}_2(\xi)-\varphi_1(\xi))\xi d\xi\right) = 1. \tag{12}$$

2. ALGORITHM OF SOLUTION OF THE PROBLEM

Let us first find wetting angles θ_1 and θ_2 (angles between the tangents to the curves determining the given surfaces and the tangents to the lateral surface profile of the liquid bridge at points ξ_1 and ξ_2, respectively). The expressions for the cosines of these angles have the form

$$\cos(\theta_i) = \cos(\arctan(w_i'(\xi_i)) - \arctan(\varphi_i'(\xi_i))) = \frac{1+w_i'(\xi_i)\varphi_i'(\xi_i)}{\sqrt{1+(w_i'(\xi_i))^2}\sqrt{1+(\varphi_i'(\xi_i))^2}}, \quad i = 1,2.$$

Consequently, transversality conditions (6), (7) yield $\cos(\theta_i) = \alpha_{i0}$, $i = 1, 2$, i.e., the Dupré–Young conditions [9] (formula (1.4)). It can be seen that, when the given surfaces are parallel planes, we obtain the expressions given in [1].

To construct the effective algorithm for solving problem (4)–(12), we perform the normalization to quantity ξ_* as follows:

(i) new independent variable $\eta = \xi/\xi_*$;

(ii) new sought functions $v_i(\eta) = w_i(\xi)/\xi_*$, $i = 1, 2$; and

(iii) modified given functions $\psi_1(\eta) = \varphi_1(\xi)/\xi_*$, $\hat{\psi}_2(\eta) = h/\xi_* + \varphi_2(\xi)/\xi_* = H + \psi_2(\eta)$.

Let us introduce notation $b = B(\xi_*)^2$ for the modified Bond number and $M = \mu\xi_*$ for the modified Lagrange multiplier.

In the new variables, Eqs. (4) and (5) take the form

$$\frac{d}{d\eta}\left(\frac{\eta v_1'(\eta)}{\sqrt{1+(v_1'(\eta))^2}}\right) = b(v_1(\eta)-\psi_1(\eta))\eta + M\eta, \quad 1 < \eta < \eta_1, \tag{13}$$

$$\frac{d}{d\eta}\left(\frac{\eta v_2'(\eta)}{\sqrt{1+(v_2'(\eta))^2}}\right) = b(\hat{\psi}_2(\eta)-v_2(\eta))\eta - M\eta, \quad 1 < \eta < \eta_2. \tag{14}$$

Integrating these equations, we obtain

$$\frac{\eta v_1'(\eta)}{\sqrt{1+(v_1'(\eta))^2}} = b\int_1^\eta (v_1(s)-\psi_1(s))sds + \frac{M(\eta^2-1)}{2} + C_1, \tag{15}$$

$$\frac{\eta v_2'(\eta)}{\sqrt{1+(v_2'(\eta))^2}} = b\int_1^\eta (\hat{\psi}_2(s)-v_2(s))sds - \frac{M(\eta^2-1)}{2} + C_2. \tag{16}$$

Passing in these relations to the limit $\eta \to 1$ taking into account conditions (11), we obtain integration constants C_1 and C_2: $C_1 = -1$ and $C_2 = 1$. Dividing both parts of relations (15) and (16) by η, we reduce these equations to the forms

$$\frac{v_1'(\eta)}{\sqrt{1+(v_1'(\eta))^2}} = \frac{1}{\eta}\left[b\int_1^\eta (v_1(s)-\psi_1(s))sds + \frac{M(\eta^2-1)}{2} - 1\right] \equiv -\Phi_1(\eta), \tag{17}$$

$$\frac{v_2'(\eta)}{\sqrt{1+(v_2'(\eta))^2}} = \frac{1}{\eta}\left[b\int_1^{\eta}(\hat{\psi}_2(s)-v_2(s))sds - \frac{M(\eta^2-1)}{2}+1\right] \equiv \Phi_2(\eta). \tag{18}$$

Auxiliary functions $\Phi_1(\eta)$ and $\Phi_2(\eta)$ introduced above must satisfy inequalities $0 < \Phi_1(\eta) \le 1$, $\eta \in [1, \eta_1]$, $0 < \Phi_2(\eta) \le 1$, $\eta \in [1, \eta_2]$ to ensure the required signs of functions $v_1'(\eta)$ and $v_2'(\eta)$ (see above). Solving Eqs. (17) and (18) with respect to the derivatives, we obtain the following equations:

$$\frac{dv_1}{d\eta} = -\frac{\Phi_1(\eta)}{\sqrt{1-(\Phi_1(\eta))^2}}, \quad \frac{dv_2}{d\eta} = \frac{\Phi_2(\eta)}{\sqrt{1-(\Phi_2(\eta))^2}}. \tag{19}$$

These equations imply that

$$\left.\frac{dv_1}{d\eta}\right|_{\eta=1} = -\infty, \quad \left.\frac{dv_2}{d\eta}\right|_{\eta=1} = +\infty,$$

i.e., the fulfillment of verticality conditions for the tangent at the neck (11). In the vicinity of point $\eta = 1$, functions $\Phi_1(\eta)$ and $\Phi_2(\eta)$ can be written in the form $\Phi_i(\eta) = 1 + O(\eta - 1)$, $i = 1, 2$; therefore, the singularities on the right-hand sides of Eqs. (19) are integrable and we can obtain the following expressions for the sought functions $v_1(\eta)$ and $v_2(\eta)$:

$$v_1(\eta) = \int_{\eta}^{\eta_1}\frac{\Phi_1(s)ds}{\sqrt{1-(\Phi_1(s))^2}} + \psi_1(\eta_1), \tag{20}$$

$$v_2(\eta) = H + \psi_2(\eta_2) - \int_{\eta}^{\eta_2}\frac{\Phi_2(s)ds}{\sqrt{1-(\Phi_2(s))^2}}, \tag{21}$$

while analogs of conditions for the contact of the liquid bridge with the bottom and top are fulfilled: $v_1(\eta_1) = \psi_1(\eta_1)$ and $v_2(\eta_2) = H + \psi_2(\eta_2)$. Satisfying the analog of condition (10), we arrive at the relation

$$H = \psi_1(\eta_1) - \psi_2(\eta_2) + \int_1^{\eta_1}\frac{\Phi_1(s)ds}{\sqrt{1-(\Phi_1(s))^2}} + \int_1^{\eta_2}\frac{\Phi_2(s)ds}{\sqrt{1-(\Phi_2(s))^2}}. \tag{22}$$

The expression for function $v_2(\eta)$ then takes the form

$$v_2(\eta) = \psi_1(\eta_1) + \int_1^{\eta_1}\frac{\Phi_1(s)ds}{\sqrt{1-(\Phi_1(s))^2}} + \int_1^{\eta}\frac{\Phi_2(s)ds}{\sqrt{1-(\Phi_2(s))^2}}. \tag{23}$$

Using relations (19), we can write transversality conditions (6) and (7) in the form

$$\sqrt{1-(\Phi_i(\eta_i))^2} + (-1)^i\psi_i'(\eta_i)\Phi_i(\eta_i) = \alpha_{i0}\sqrt{1+(\psi_i'(\eta_i))^2}, \quad i = 1, 2.$$

Solving these equations for quantities $\Phi_1(\eta_1)$ and $\Phi_2(\eta_2)$, we obtain

$$\Phi_i(\eta_i) = \alpha_i(\eta_i), \quad \alpha_i(\eta_i) = \frac{\sqrt{1-(\alpha_{i0})^2+(-1)^i\alpha_{i0}\psi_i'(\eta_i)}}{\sqrt{1+(\psi_i'(\eta_i))^2}}, \quad i = 1, 2. \tag{24}$$

After the substitution of expressions for $\Phi_1(\eta_1)$ and $\Phi_2(\eta_2)$ into these relations, we obtain the following equations for η_1 and η_2:

$$\frac{1}{2}M\eta_1^2 + \alpha_1(\eta_1)\eta_1 - \left[1+\frac{1}{2}M - b\int_1^{\eta_1}(v_1(s)-\psi_1(s))sds\right] = 0, \tag{25}$$

$$\frac{1}{2}M\eta_2^2 + \alpha_2(\eta_2)\eta_2 - \left[1+\frac{1}{2}M + b\int_1^{\eta_2}(\hat{\psi}_2(s)-v_2(s))sds\right] = 0. \tag{26}$$

Let us write condition of volume conservation (12) in the new variables:

$$\xi_*^3\left(\int_1^{\eta_1}(v_1(s)-\psi_1(s))sds + \int_1^{\eta_2}(\hat{\psi}_2(s)-v_2(s))sds + \int_0^1(\hat{\psi}_2(s)-\psi_1(s))sds\right) = \frac{1}{2\pi}. \tag{27}$$

Integrating by parts, we transform this relation to the form

$$\xi_* = \left\{\pi\left[\int_1^{\eta_1}\frac{\Phi_1(s)s^2ds}{\sqrt{1-(\Phi_1(s))^2}} + \int_1^{\eta_2}\frac{\Phi_2(s)s^2ds}{\sqrt{1-(\Phi_2(s))^2}} + \int_0^{\eta_1}\psi_1'(s)s^2ds - \int_0^{\eta_2}\psi_2'(s)s^2ds\right]\right\}^{-1/3}. \tag{28}$$

Thus, we have derived all the relations required for solving the problem.

Let the Bond number be a small parameter of the problem in question. We propose the following algorithm of its solution for preset values of α_{10}, α_{20}, and $\hat{h}$.

We organize the iterative process to small parameter b (main iterative process).

2.1. First Iteration (Construction of the Zeroth Approximation)

At the first iteration, we assume that $b = 0$ (we construct the approximate solution to the problem disregarding the gravity force). We specify the value of parameter M from the range of admissible values and define functions $\Phi_1(\eta)$ and $\Phi_2(\eta)$ using formulas (17) and (18). We consider that admissible values of parameter M are those for which each of Eqs. (25), (26) has at least one positive root greater than unity. For positive admissible values, there is only one such root for each equation, while for negative admissible values, each equation has two such roots. In the latter case, to one value of parameter M correspond four solutions to the problem, which are determined by the choice of roots of Eqs. (25) and (26). There are the following combinations of chosen roots: variant (+ +), i.e., maximal roots of these equations; (+ –) are the maximal root of Eq. (25) and the minimal root of Eq. (26); in variant (– +), conversely, there are the minimal root of Eq. (25) and the maximal root of Eq. (26); and, finally, (– –); i.e., both roots are minimal. Further, we solve nonlinear equations (25) and (26) for quantities η_1 and η_2. For this purpose, we reduce the solution of the nonlinear equations to the solution of a sequence of quadratic equations by the iterative method (with an auxiliary iterative process required only for constructing the zeroth approximation to initiate the main iterative process and to account for the shapes of the given surfaces between which the liquid bridge is located). Namely, we believe that $f_1'(r) = 0$, $f_2'(r) = 0$; then, $\alpha_i(\eta_i) = \sqrt{1-(\alpha_{i0})^2}$, $i = 1, 2$ (liquid bridge between the planes; Eqs. (25) and (26) are quadratic equations) and find their positive roots, which are greater than unity. We determine quantity ξ_* using formula (28). We are using these found values of roots η_1 and η_2 for calculating $\alpha_i(\eta_i)$, $i = 1, 2$. We then again solve quadratic equations (25) and (26) and find ξ_* using formula (28). We continue this process until the difference in the values of the roots at two sequential steps of the auxiliary iterative process becomes smaller than a preset value determining the accuracy of calculations for the zeroth approximation. We find the value of H using formula (22) and functions $v_1(\eta)$ and $v_2(\eta)$ using formulas (20) and (23); finally, we determine ξ_1, ξ_2, h, $w_1(\xi)$, $w_2(\xi)$, θ_1, and θ_2. This completes the construction of the zeroth approximation for given values of α_{i0}, $i = 1, 2$, and for the chosen value of parameter M. Up to four different profiles can correspond to one value of parameter M.

It we wish to restrict ourselves to finding the zeroth approximation, we iterate over all admissible values of parameter M, construct the dependence of the liquid bridge height on parameter M, and find the solution corresponding to the given value of the height.

2.2. Second and Next Iterations of the Main Iterative Process

If, however, we do not confine our analysis to investigation of a liquid bridge in zero gravity, we continue calculations for the chosen value of parameter M. Namely, we find the value of parameter $b = B(\xi_*)^2$ and determine new auxiliary functions $\Phi_1(\eta)$ and $\Phi_2(\eta)$ by formulas (17) and (18) using for calculations functions v_1, v_2, ψ_1, and ψ_2 obtained at the first iteration. Equations (25) and (26) at the second iteration are quadratic equations with respect to η_1 and η_2 with constant coefficients, because we calculate these coefficients using the values obtained at the previous iteration. We find η_1, η_2, ξ_*, H, $v_1(\eta)$, and $v_2(\eta)$, as well as ξ_1, ξ_2, h, $w_1(\xi)$, and $w_2(\xi)$, and then we find the new value of parameter $b = B(\xi_*)^2$ and we perform the third iteration analogously, and so on until the differences in the values of η_1 and η_2 at two sequential steps of the main iterative process become smaller than a certain value determining the accuracy of the solution to the problem.

We then perform all the calculations described above for each admissible value of parameter M, construct the dependence of liquid bridge height h on parameter M, and find the solution to the problem that corresponds to the given value of the bridge height. The maximum number of such solutions is four.

3. EXAMPLE OF CALCULATION OF A LIQUID BRIDGE BETWEEN TWO SPHERES

Let us use the above algorithm for calculating the particular case of a vertical catenoidal liquid bridge between two spheres. Let the bottom be a sphere of radius $R_1 = 6$: $\varphi_1(\xi) = -R_1 + \sqrt{R_1^2 - \xi^2}$ and the top be a sphere of radius $R_2 = 8$: $\hat{\varphi}_2(\xi) = h + \phi_2(\xi)$, $\phi_2(\xi) = R_2 - \sqrt{R_2^2 - \xi^2}$. We perform calculations for the Bond number equal to 0.25, $\alpha_{10} = 0.5$, $\alpha_{20} = 0.7$, and carry out the first and second iterations. We present the results of calculations after the first step of the main iterative process since the differences in the results are small, and the profile graphs practically coincide. Figure 2 illustrates this situation. We choose variant (+ +) because the values of parameter b characterizing the radius of the neck in this variant are maximal.

It can be seen that the main iterative process converges well. As regards the convergence of the auxiliary iterative process, its four steps yield an error of 0.5%. Let us introduce notation $h_0 = H\xi_*$, where the values of H and ξ_* are taken after four steps.

Figure 3 shows the dependence of the liquid bridge height h_0 (the distance between the spheres) on parameter M. For admissible positive values of parameter M, we have a single curve, while, for admissible

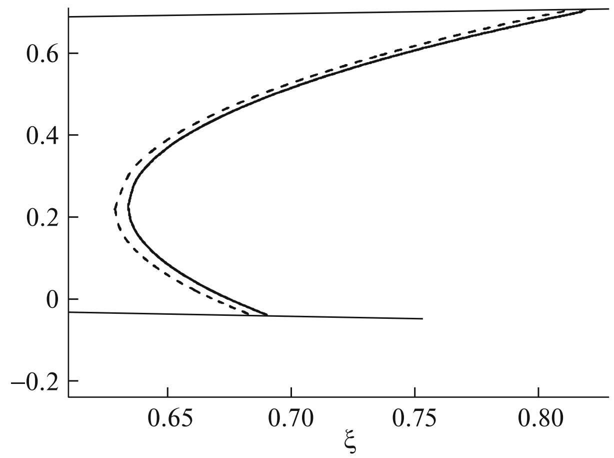

Fig. 2. Liquid bridge profiles after the first step of the main iterative process (solid curve) and after the second step (dashed curve) for $\alpha_1 = 0.5$, $\alpha_2 = 0.7$, $M = -0.01$, $R_1 = 6$, $R_2 = 8$, $B = 0.25$, and $b = 0.1$. Variant (+ +).

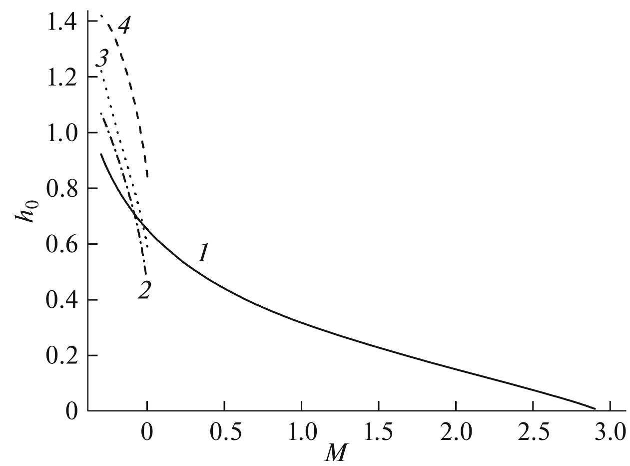

Fig. 3. Dependence of liquid bridge height h_0 on parameter M. Curves *1–4* correspond to variants (+ +), (+ –), (– +), and (– –) of the choice of the values of roots, respectively.

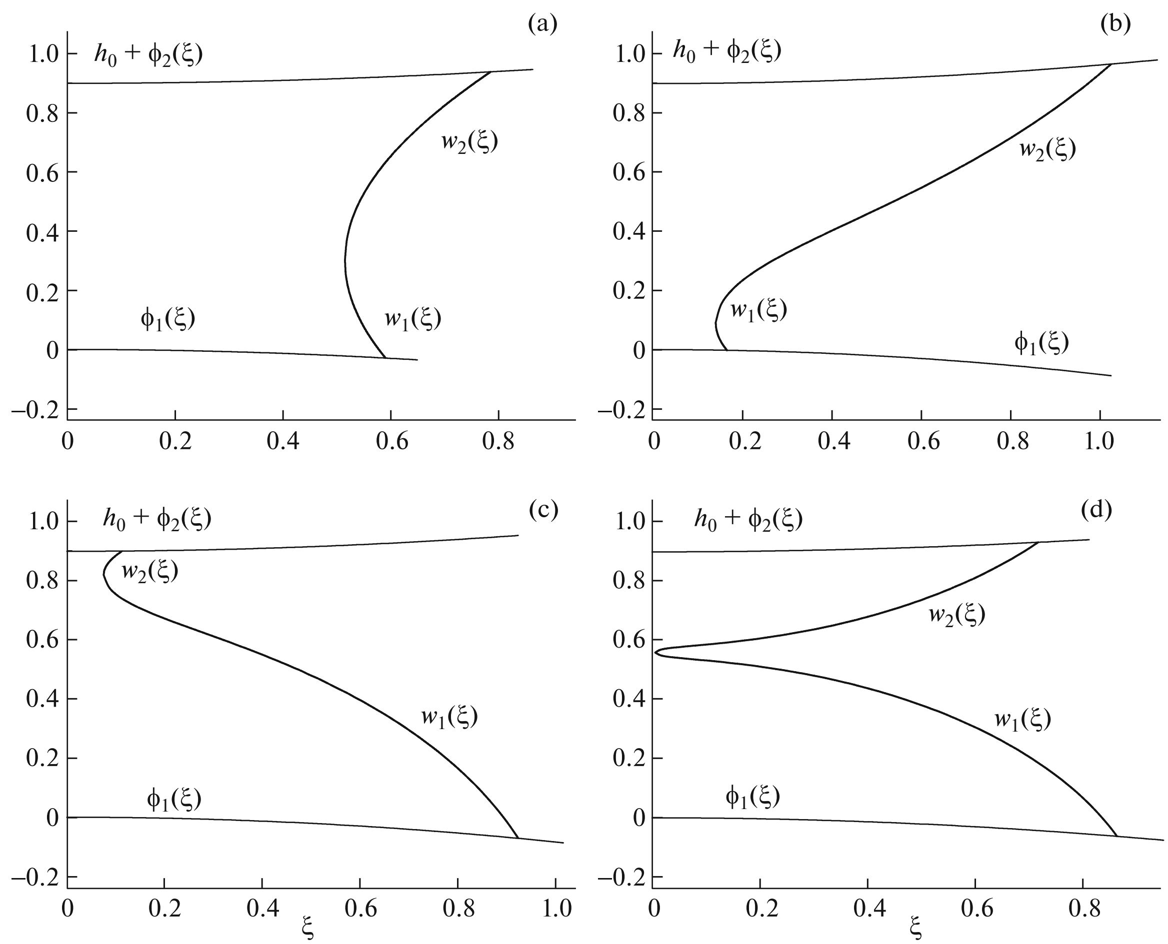

Fig. 4. Four different liquid bridge profiles corresponding to a single value of the bridge height: (a) variant (+ +), $M = -0.284$; (b) (+ –), $M = -0.185$; (c) (– +), $M = -0.14$, and (d) (– –), $M = -0.013$.

negative values of M, we obtain four different curves corresponding to four variant of the choice of roots of Eqs. (25) and (26). There exists the maximal value of the liquid bridge height (there are no solutions for height exceeding this value). There are intervals of height variation, which correspond to the existence of one, two, three, and four solutions. In addition, it can be seen from this figure that, in contrast to a liquid bridge between two parallel solid surfaces, there exists in this case a finite positive value of parameter M corresponding to the point of tangency of the spheres.

Finally, Fig. 4 shows four different profiles of the lateral surface of the liquid bridge between the spheres, which correspond to a single value of liquid bridge height $h_0 = 0.9$ and four different values of parameter M. It should be noted that the curve in Fig. 4a corresponding to variant (+ +) correlates with the photographs obtained during the experiment and given in [6], while the remaining three graphs reflect other theoretically possible profiles.

CONCLUSIONS

We have proposed an effective algorithm for solving problem of determining the shape of the lateral surface of a vertical catenoidal liquid bridge between solid convex small-curvature surfaces taking into account the gravity force. A variational formulation of the problem has been given. The solution is found by the iterative method under the assumption of smallness of the Bond number. The iterative process is started from the case of a liquid bridge between parallel planes. The lack of uniqueness of the solution to the problem has been discovered. It has been established that the maximum number of different solutions for a fixed set of given parameters is four. By way of example, an approximate solution to the problem of the shape of a liquid bridge between two spheres has been constructed. The dependence of the number of solutions on the bridge height has been investigated. Four different profiles of the bridge lateral surface, which correspond to a certain value of the bridge height, have been presented.

CONFLIICT OF INTEREST

The authors declare that they have no conflicts of interest.

REFERENCES

1. E. V. Galaktionov, N. E. Galaktionova, and E. A. Tropp, Tech. Phys. **62** (10), 1482 (2017). https://doi.org/10.1134/S1063784217100115
2. E. V. Galaktionov, N. E. Galaktionova, and E. A. Tropp, J. Phys.: Conf. Ser. **1400** (4), 044025 (2019). https://doi.org/10.1088/1742-6596/1400/4/044025
3. P. I. Antonov, L. M. Zatulovskiy, A. S. Kostygov, D. I. Levinzon, S. P. Nikanorov, V. V. Peller, V. A. Tatarchenko, and V. S. Yuferev, *Obtaining Profiled Single Crystals and Articles by Stepanov's Method*, Ed. by V. R. Regel (Nauka, Leningrad, 1981) [in Russian].
4. M. Haynes, S. B. G. O'Brien, and E. S. Benilov, Phys. Fluids **28**, 042107 (2016). https://doi.org/10.1063/1.4946001
5. G. Gagneux and O. Millet, Transp. Porous Media **105**, 117 (2014). https://doi.org/10.1007/s11242-014-0363-y
6. H. N. G. Nguyen, O. Millet, and G. Gagneux, Continuum Mech. Thermodyn. **31**, 225 (2019). https://doi.org/10.1007/s00161-018-0658-2
7. P. I. C. Teixeira and M. A. C. Teixeira, J. Phys.: Condens. Matter **32** (3), 034002 (2020). https://doi.org/10.1088/1361-648X/ab48b7
8. E. Bendito, M. J. Bowick, and A. Medina, J. Geom. Symmetry Phys. **33**, 27 (2014). https://doi.org/10.7546/jgsp-33-2014-27-45
9. A. D. Myshkis, V. G. Babskii, N. D. Kopachevskii, L. A. Slobozhanin, and A. D. Tyuptsov, *Low-Gravity Fluid Mechanics* (Springer, Berlin, 1987). https://www.springer.com/gp/book/9783642709661.

Translated by N. Wadhwa